JOURNAL OF SOLID STATE CHEMISTRY **138,** 365–368 (1998)
ARTICLE NO. SC987780

BRIEF COMMUNICATION

Synthesis, Structure, and Properties of $Tl_2(MoO_3)_3PO_3CH_3$

William T. A. Harrison,[1,*] Laurie L. Dussack,† and Allan J. Jacobson†

*Department of Chemistry, University of Western Australia, Nedlands, Western Australia 6907, Australia; and †Department of Chemistry, University of Houston, Texas 77204–5641

Received September 24, 1997; accepted February 11, 1998

Synthetic $Tl_2(MoO_3)_3PO_3CH_3$ is built up from infinite sheets of distorted octahedral MoO_6 groups, sharing vertices. These octahedral layers are "capped" by P–CH_3 entities (as tetrahedral methylphosphonate $PO_3CH_3^{2-}$ groups) on one face of each Mo/O sheet. Interlayer thallium cations provide charge compensation for the anionic sheets. Physical data are described. Crystal data: $Tl_2(MoO_3)_3PO_3CH_3$, $M_r = 934.56$, rhombohedral, space group $R3$ (No. 146), $a = 7.281$ (1) Å, $c = 18.932$ (2) Å, $V = 869.0$ (3) Å^3, $Z = 3$, $R(F) = 4.76\%$, $R_w(F) = 5.35\%$ [824 observed reflections with $I > 3\sigma(I)$].

INTRODUCTION

We have recently described the synthesis and characterization of a family of layered materials that share a common structural motif of three rings and six rings of vertex-sharing VO_6, MoO_6, or WO_6 octahedra (1–8). The same octahedral arrangement occurs in one layer of the hexagonal tungsten oxide (HTO, or hex-WO_3) structure (9). In the layered phases, the octahedral sheets are "capped" by Se atoms (as pyramidal SeO_3^{2-} groups) or P–CH_3 entities (as tetrahedral methylphosphonate groups). These phases may be classified according to layer stacking sequence, type of capping, and octahedral distortion mode (7).

In this paper we report the hydrothermal synthesis, single-crystal structure, and some properties of thallium molybednum methylphosphonate, $Tl_2(MoO_3)_3PO_3CH_3$, which is isostructural with $M_2(MoO_3)_3PO_3CH_3$ (M = Cs, Rb) (3).

EXPERIMENTAL

$Tl_2(MoO_3)_3PO_3CH_3$ was prepared hydrothermally from 0.975 g Tl_2CO_3 (4.17 mmol Tl), 0.600 g MoO_3 (4.17 mmol Mo), 0.400 g $CH_3PO_3H_2$ (4.17 mmol P), and 6 ml deionized water. These components were enclosed in a 23-ml-capacity Teflon-lined hydrothermal bomb and heated to 180°C for 48 h. After slow cooling to ambient over 16 h, the bomb was opened and the solids recovered by vacuum filtration. The biphasic product consisted of an unidentified yellow powder and pale bluish rhombs (maximum linear dimension, ~2 mm) of the title compound. The yellow powder was completely dissolved by sonicating this mixture in 1:3 $HNO_3:H_2O$ solution for 5 to 10 min, resulting in a 36% yield of single crystals of $Tl_2(MoO_3)_3PO_3CH_3$. The kinetics of this hydrothermal reaction appear to be complex, with the yield of $Tl_2(MoO_3)_3PO_3CH_3$ peaking after about 48 h and then sharply declining (10).

Powder diffraction data for a thoroughly ground sample of $Tl_2(MoO_3)_3PO_3CH_3$ were collected on a Scintag D5000 powder diffractometer (Cu$K\alpha$ radiation, $\lambda = 1.5418$ Å, $T = 25$°C). After software "stripping" of the $K\alpha_2$ component, the program ERACEL (11) indexed the data (Table 1) on a rhombohedral cell with $a = 7.284$ (2) Å and $c = 18.932$ (4) Å ($V = 869.9$ Å^3) relative to the $K\alpha_1$ wavelength ($\lambda = 1.54056$ Å). Thermogravimetric analysis (ramp at 5°C/min under flowing N_2 gas) was carried out on a Dupont 2950 instrument. Infrared spectroscopic data (KBr pellet method) were collected on a Galaxy FTIR 5000 series spectrometer.

The crystal structure of $Tl_2(MoO_3)_3PO_3CH_3$ was established from single-crystal diffraction data: irregular lump, $\sim 0.3 \times 0.3 \times 0.4$ mm; Siemens P4 diffractometer; trigonal/rhombohedral unit cell from 21 peaks ($15° < 2\theta < 25°$); data collection range, $2° < 2\theta < 70°$; hkl limits, $-11 \rightarrow 5$, $0 \rightarrow 11$, $-1 \rightarrow 30$; 1393 data; empirical absorption correction from ψ scans (min, max equivalent transmission factors = 0.010, 0.053); $R_{int} = 7.15\%$. The starting atomic model in space group $R3$ (No. 146) was taken from the structure of $Cs_2(MoO_3)_3PO_3CH_3$ (Tl replacing Cs) (3). Refinement with CRYSTALS (12) proceeded satisfactorily to convergence (Table 2). No protons could be located.

[1] To whom correspondence should be addressed. E-mail: wtah@chem.uwa.edu.au.

0022-4596/98 $25.00

TABLE 1
Powder Data for $Tl_2(MoO_3)_3PO_3CH_3$

h	k	l	d_{obs} (Å)	d_{calc} (Å)	Δd	I_{rel}
0	0	3	6.304	6.311	− 0.007	15
1	0	1	5.979	5.985	− 0.005	23
0	1	2	5.247	5.249	− 0.002	10
1	0	4	3.788	3.786	0.002	4
1	1	0	3.644	3.642	0.002	18
0	1	5	3.247	3.246	0.001	65
0	0	6	3.155	3.155	0.000	100
0	2	1	3.112	3.111	0.001	10
2	0	2	2.992	2.992	0.000	42
0	2	4	2.625	2.625	0.001	9
1	0	7	2.486	2.486	0.000	16
2	0	5	2.423	2.423	0.000	7
1	1	6	2.385	2.385	0.000	9
2	1	1	2.365	2.366	0.000	4
1	2	2	2.312	2.312	0.000	8
0	1	8	2.216	2.216	0.000	6
3	0	0	2.103	2.103	0.001	7
0	2	7	2.053	2.053	0.000	2
2	1	5	2.017	2.018	0.000	13
3	0	3	1.995	1.995	0.000	13

Supplementary crystallographic data are available from the authors.

RESULTS

Crystal Structure

Final atomic positional and thermal parameters for $Tl_2(MoO_3)_3PO_3CH_3$ are listed in Table 3, with selected geometrical data in Table 4. $Tl_2(MoO_3)_3PO_3CH_3$ is a new layered phase build up from vertex-sharing MoO_6 and PO_3CH_3 units, fused together via Mo–O–Mo and Mo–O–P bonds. Interlayer Tl^+ cations complete the crystal structure (Figs. 1, 2).

The thallium cations, both of site symmetry 3, serve to link adjacent anionic sheets by way of Tl–O bonds. Tl(1) forms a distorted trigonal prism with its six O atom neighbors, with d_{av}(Tl–O) = 3.02 Å. Tl(2) is 12-coordinate [d_{av}(Tl–O) = 3.07 Å]. Bond valence sum (BVS) calculations (13) for the thallium cations yielded BVS[Tl(1)] = 0.60 and BVS[Tl(2)] = 1.06 (expected = 1.00), indicating a significant degree of "underbonding" for Tl(1), which may account for the large thermal motion of this species. The MoO_6

TABLE 2
Crystallographic Parameters for $Tl_2(MoO_3)_3PO_3CH_3$

Empirical formula	$Tl_2Mo_3PO_{12}CH_3$
Formula weight	934.56
Crystal system	Rhombohedral
a	7.281(1) Å
c	18.932(2) Å
V	869.0(3) Å^3
Z	3
Space group	$R3$ (No. 146)
T	25(2)°C
λ (Mo$K\alpha$)	0.71073 Å
ρ_{calc}	5.36 g/cm^3
μ	312.8 cm^{-1}
Total data	1393
Observed data[a]	824
Parameters	60
$R(F)$[b]	4.76
$R_w(F)$[c]	5.35

[a] $I > 3\sigma(I)$ after data merging to 922 reflections.
[b] $R = 100 \times \sum ||F_o| - F_c|| / \sum |F_o|$.
[c] $R_w = 100 \times [\sum w(|F_o| - |F_c|)^2 / \sum w|F_o|^2]^{1/2}$, with w_i described by a Chebychev polynomial.

TABLE 3
Atomic Positional/Thermal Parameters for $Tl_2(MoO_3)_3PO_3CH_3$

Atom	x	y	z	U_{eq}[a]
Tl(1)	0	0	0.17511 (9)	0.0526
Tl(2)	1/3	2/3	0.22661 (8)	0.0284
Mo(1)	0.0067 (1)	0.5404 (1)	0.05744 (9)	0.0131
P(1)	− 1/3	1/3	0.1901 (2)	0.0135
O(1)	0.075 (2)	0.541 (1)	− 0.0294 (5)	0.0199
O(2)	0.215 (1)	0.797 (1)	0.0885 (5)	0.0194
O(3)	− 0.213 (1)	0.582 (1)	0.0468 (5)	0.0178
O(4)	− 0.102 (1)	0.453 (1)	0.1645 (5)	0.0183
C(1)	− 1/3	1/3	0.282 (1)	0.0160

[a] U_{eq} (Å^2) = 1/3 [$U_1 + U_2 + U_3$].

TABLE 4
Selected Bond Distances (Å) and Angles (Degrees) for $Tl_2(MoO_3)_3PO_3CH_3$

Tl(1)–O(1) × 3	2.93(1)	Tl(1)–O(2) × 3	3.11 (1)
Tl(2)–O(1) × 3	2.96 (1)	Tl(2)–O(2) × 3	3.05 (1)
Tl(2)–O(3) × 3	3.30 (1)	Tl(2)–O(4) × 3	2.985 (9)
Mo(1)–O(1)	1.72(1)	Mo(1)–O(2)	1.815 (9)
Mo(1)–O(2)	2.113 (9)	Mo(1)–O(3)	1.780 (8)
Mo(1)–O(3)	2.106 (8)	Mo(1)–O(4)	2.153 (9)
P(1)–O(4) × 3	1.539(9)	P(1)–C(1)	1.74(2)
O(1)–Mo(1)–O(2)	102.5 (4)	O(1)–Mo(1)–O(2)	90.6 (4)
O(2)–Mo(1)–O(2)	87.1 (5)	O(1)–Mo(1)–O(3)	100.0 (4)
O(2)–Mo(1)–O(3)	102.8 (4)	O(2)–Mo(1)–O(3)	163.4 (4)
O(1)–Mo(1)–O(3)	87.6 (4)	O(2)–Mo(1)–O(3)	163.3 (4)
O(2)–Mo(1)–O(3)	79.5 (3)	O(3)–Mo(1)–O(3)	88.2 (5)
O(1)–Mo(1)–O(4)	164.8 (4)	O(2)–Mo(1)–O(4)	89.6 (4)
O(2)–Mo(1)–O(4)	80.7 (4)	O(3)–Mo(1)–O(4)	86.0 (4)
O(3)–Mo(1)–O(4)	78.6 (4)	O(4)–P(1)–O(4)	110.6 (4)
O(4)–P(1)–C(1)	108.4 (4)	Mo(1)–O(2)–Mo(1)	132.5 (6)
Mo(1)–O(3)–Mo(1)	148.8 (5)	Mo(1)–O(4)–P(1)	126.9 (5)

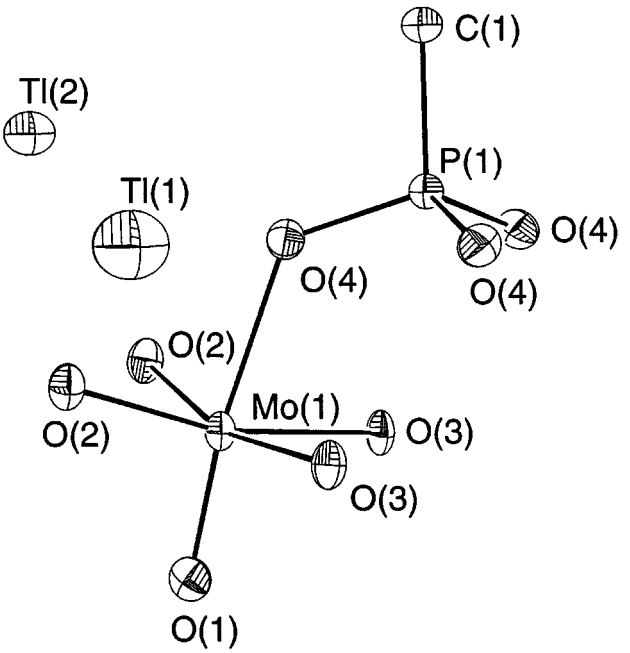

FIG. 1. View of the building unit of $Tl_2(MoO_3)_3PO_3CH_3$ showing the atom-labeling scheme (50% thermal ellipsoids).

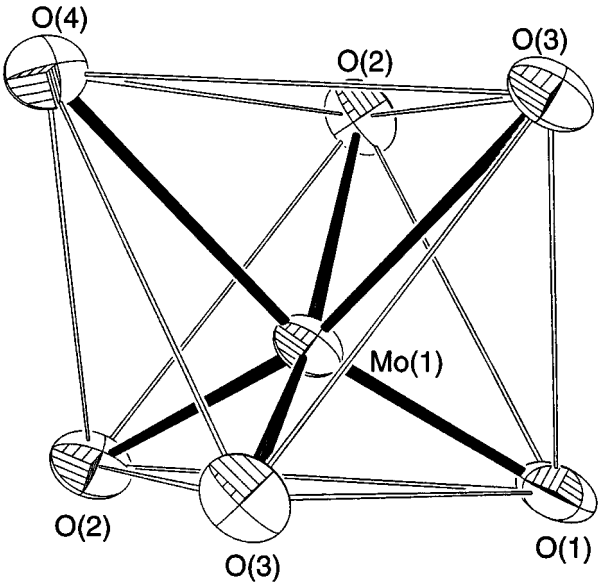

FIG. 3. Detail showing the (three short + three long) Mo–O bond distance distribution in the MoO_6 octahedron in $Tl_2(MoO_3)_3PO_3CH_3$.

grouping (Fig. 3) shows a distinctive distortion mode, with the Mo atom making a nominal displacement by ~ 0.33 Å from the geometric center of its octahedron toward an octahedral face ("local [111] distortion" (3)). This results in three short ($d < 1.82$ Å) Mo–O vertices, each of which is *trans* to a long ($d > 2.10$ Å) Mo–O bond. A BVS of 6.02 results for Mo (expected value = 6.00 for Mo^{VI}). The P–C bond of the PO_3CH_3 group occupies a threefold axis, and overall, this tetrahedral grouping has typical geometrical parameters (3, 7).

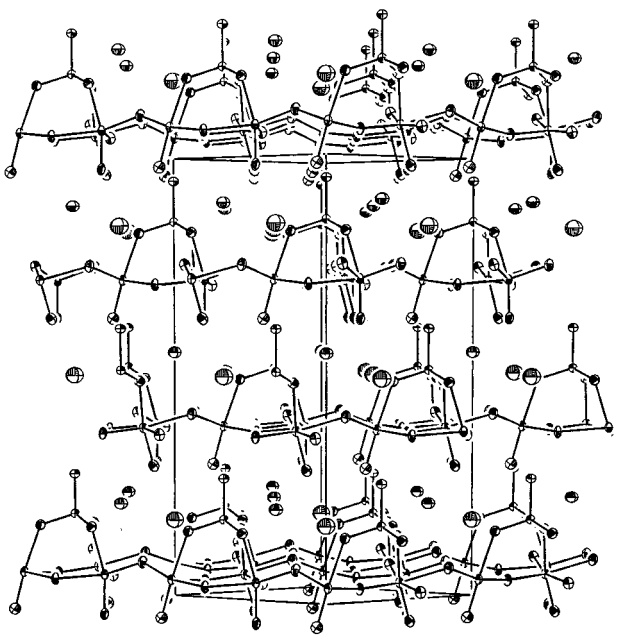

FIG. 2. Unit-cell packing in $Tl_2(MoO_3)_3PO_3CH_3$ viewed normal to [110] showing the layered crystal structure, with PO_3CH_3 capping occurring on one side of the octahedral Mo/O sheets. Tl–O bonds are omitted for clarity.

The polyhedral connectivity in $Tl_2(MoO_3)_3PO_3CH_3$ results in infinite sheets of vertex-sharting MoO_6 octahedra, arranged into a three-ring/six-ring motif lying normal to [0001]. All the interoctahedral bonds consist of a short and a long (Mo=O-Mo) linkage, with an average bond angle of 140.7°. The octahedral sheets are significantly puckered, with the long in-layer Mo–O(2) and Mo–O(3) bonds canted from the (110) plane by $\sim 16.2°$ and $\sim 5.5°$, respectively. The two remaining Mo–O vertices are approximately aligned along [0001]. The short Mo–O(1) bond is terminal; all these bonds point in the same direction in the polar unit cell. The Mo–O(4) bond *trans* to Mo–O(1) forms part of a Mo–O–P linkage; thus all the methylphosphonate groups occur on one face of the octahedral Mo/O sheets. The interlayer separation of the resulting anionic $[(MoO_3)_3PO_3CH_3]^{2-}$ sheets is ~ 6.31 Å. The rhombohedral crystal symmetry dictates an *ABCABC*... repeat motif for the stacking of the sheets along [0001]. All the methylphosphonate groups point toward a six-ring window in the adjacent octahedral sheet. Because the $[(MoO_3)_3PO_3CH_3]^{2-}$ sheets are offset (7), there are no channels in the [0001] direction comparable to the infinite six-ring channels seen in hex-WO_3 (9).

Physical Data

TGA for $Tl_2(MoO_3)_3PO_3CH_3$ revealed thermal stability until $\sim$435°C (onset of a $\sim$3.3% a weight loss) followed by a second weight loss of $\sim$2.0% at $\sim$550°C. Powder diffraction showed that the blackish-blue post-TGA residue contained poorly crystalline MoO_2 (14) and, by implication, amorphous Tl/Mo/P/O component(s), suggesting that the decompsotion pathway is complex.

Infrared data for $Tl_2(MoO_3)_3PO_3CH_3$ are shown in Fig. 4. The spectrum is similar to those previously observed for $Cs_2(MoO_3)_3PO_3CH_3$ and $Rb_2(MoO_3)_3PO_3CH_3$ (3). Prominent peaks include CH_3 stretching and bending modes (2933 and 1414 cm^{-1}, respectively), the P–C stretch 1305 cm^{-1}), octahedral Mo–O modes (850 cm^{-1}, broad feature at 675 cm^{-1}), and P–O modes (1016 and 904 cm^{-1}).

DISCUSSION

$Tl_2(MoO_3)_3PO_3CH_3$ is another member of the $M_2(MoO_3)_3PO_3CH_3$ (M = Cs, Rb) family of layered phases (3) and is essentially isostructural with these materials. The structural effect, if any, of the Tl^+ lone pair is hard to gauge in this structure. Its two positions in the interlayer region of the sturcture are similar to those of the Cs^+ and Rb^+ species in the isostructural phases (3). The "underbonded" situation of the trigonal-prismatically coordinated Tl(1) cation was also observed for the equivalent Cs(1) and Rb(1) species. The interlayer separation of 6.31 Å in the thallium phase is actually somewhat smaller than that observed for the cesium (6.67 Å) and rubidium (6.68 Å) phases.

The Mo cation in $Tl_2(MoO_3)_3PO_3CH_3$ exhibits a (three-short + three long) Mo–O bond distance distribution in its MoO_6 octahedron similar to that seen in the cesium and rubidium phases (3). The nominal Mo atom displacement of $\sim$0.33 Å in $Tl_2(MoO_3)_3PO_3CH_3$ is almost identical to the magnitudes of the displacements seen in $Cs_2(MoO_3)_3PO_3CH_3$ (0.34 Å) and $Rb_2(MoO_3)_3PO_3CH_3$ (0.34 Å) (3). The distortion (nominal shift of the cation in its octahedron) of a d^0 species may be understood in terms of a second-order Jahn–Teller effect (15), although the magnitude and direction of such a distortion are difficult to predict (16). This (three short + three long) Mo–O octahedral bond distribution, which also occurs in the layered phase $BaMoO_3SeO_3$ (17), is less common than the (two short + two intermediate + two long) distribution seen in many Mo^{VI}-containing phases such as $BaMo_4O_{13} \cdot 2H_2O$ (18) or the (one short + four intermediate + one long) bond distribution seen in molybdophosphate clusters based on the Keggin ion structure (19).

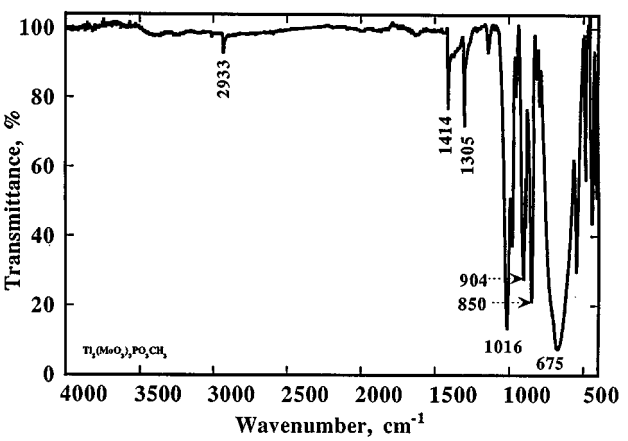

FIG. 4. Infrared spectrum of $Tl_2(MoO_3)_3PO_3CH_3$.

ACKNOWLEDGMENTS

This work is supported by the Australian Research Council and the National Science Foundation.

REFERENCES

1. J. T. Vaughey, W. T. A. Harrison, L. L. Dussack, and A. J. Jacobson, *Inorg. Chem.* **33,** 4370 (1994).
2. W. T. A. Harrison, L. L. Dussack, and A. J. Jacobson, *Acta Crystallogr. C* **51,** 2473 (1995).
3. W. T. A. Harrison, L. L. Dussack, and A. J. Jacobson, *Inorg. Chem.* **34,** 4774 (1995).
4. W. T. A. Harrison, L. L. Dussack, and A. J. Jacobson, *Inorg. Chem.* **33,** 6043 (1994).
5. W. T. A. Harrison, L. L. Dussack, and A. J. Jacobson, *Inorg. Chem.* **35,** 1461 (1996).
6. W. T. A. Harrison, L. L. Dussack, T. Vogt, and A. J. Jacobson, *J. Solid State Chem.* **120,** 112 (1995).
7. W. T. A. Harrison, L. L. Dussack, J. T. Vaughey, T. Vogt, and A. J. Jacobson, *J. Mater. Chem.* **6,** 81 (1996).
8. L. L. Dussack, W. T. A. Harrison, and A. J. Jacobson, *Mater. Res. Bull.* **31,** 249 (1996).
9. B. Gérand, G. Nowogrocki, J. Guenot, and M. Figlarz, *J. Solid State Chem.* **29,** 429 (1979).
10. L. L. Dussack, Ph.D. thesis, University of Houston, 1996.
11. J. Lauglier and A. Filhol, "Program ERACEL," Version distributed by A. LeBail, University of Le Mans, 1997.
12. D. J. Watkin, J. R. Carruthers, and P. W. Betteridge, "CRYSTALS User Guide," Chemical Crystallography Laboratory, University of Oxford.
13. I. D. Brown, *J. Appl. Crystallogr.* **29,** 479 (1996).
14. JCPDS Powder Diffraction File Card 32-0571.
15. J. K. Burdett, "Molecular Shapes," Wiley–Interscience, New York, 1980.
16. M. Kunz and I. D. Brown, *J. Solid State Chem.* **115,** 395 (1995).
17. W. T. A. Harrison, L. L. Dussack, and A. J. Jacobson, *J. Solid State Chem.* **125,** 234 (1996).
18. W. T. A. Harrison, L. L. Dussack, and A. J. Jacobson, *J. Solid State Chem.* **116,** 95 (1995).
19. J. C. A. Boeyens, G. J. McDougal, and J. van Smit, *J. Solid State Chem.* **18,** 191 (1976).